ELSEVIER

Biophysical Chemistry 128 (2007) 156–164

Biophysical Chemistry

http://www.elsevier.com/locate/biophyschem

Agonist versus antagonist induce distinct thermodynamic modes of co-factor binding to the glucocorticoid receptor

Rachel R. Kroe [a], Martha A. Baker [a], Martha P. Brown [a], Neil A. Farrow [b], Elda Gautschi [a], Jerry L. Hopkins [a], Roger R. LaFrance [a], Anthony Kronkaitis [a], Dorothy Freeman [a], David Thomson [c], Gerald Nabozny [d], Christine A. Grygon [a], Mark E. Labadia [d,*]

[a] *Department of Biologics and Biomolecular Sciences, Boehringer Ingelheim Pharmaceuticals, 900 Ridgebury Rd., Ridgefield CT 06877, United States*
[b] *Department of Structural Research, Boehringer Ingelheim Pharmaceuticals, 900 Ridgebury Rd., Ridgefield CT 06877, United States*
[c] *Department of Medicinal Chemistry, Boehringer Ingelheim Pharmaceuticals, 900 Ridgebury Rd., Ridgefield CT 06877, United States*
[d] *Department of Immunology, Boehringer Ingelheim Pharmaceuticals, 900 Ridgebury Rd., Ridgefield CT 06877, United States*

Received 30 December 2006; received in revised form 21 March 2007; accepted 24 March 2007
Available online 5 April 2007

Abstract

The glucocorticoid receptor (GR) is involved in the transcriptional regulation of genes associated with inflammation, glucose homeostasis, and bone turnover through the association with ligands, such as corticosteroids. GR-mediated gene transcription is regulated or fine-tuned via the recruitment of co-factors including coactivators and corepressors. Current therapeutic approaches to targeting GR aim to retain the beneficial anti-inflammatory activity of the corticosteroids while eliminating negative side effects. Towards achieving this goal the experiments discussed here reveal a mechanism of co-factor binding in the presence of either bound agonist or antagonist. The GR ligand binding domain (GR-LBD(F602S)), in the presence of agonist or antagonist, utilizes different modes of binding for coactivator versus corepressor. Coactivator binding to the co-effector binding pocket of GR-LBD(F602S) is driven both by favorable enthalpic and entropic interactions whereas corepressor binding to the same pocket is entropically driven. These data support the hypothesis that ligand-induced conformational changes dictate co-factor binding and subsequent *trans*-activation or *trans*-repression.

Keywords: Glucocorticoid receptor; Dexamethasone; RU-486; Isothermal titration calorimetry; Surface Plasmon Resonance; Analytical ultracentrifugation

1. Introduction

The glucocorticoid receptor (GR) is a ligand-dependent transcription factor that is a member of the nuclear receptor super-family, which includes receptors for mineralocorticoids, estrogens, progestins, androgens, thyroid hormones, and vitamin D. GR is involved in the regulation of genes associated with various functions including inflammation, glucose homeostasis, and bone turnover. GR ligands, including the corticosteroids Dexamethasone and Prednisolone, are commonly used therapeutically for the treatment of diseases such as asthma, allergic rhinitis and rheumatoid arthritis.

In its inactivated state, GR resides in the cytoplasm as a heterocomplex with several chaperone proteins including HSP90. When ligand diffuses across the cell membrane and binds to GR, HSP90 and the other chaperone proteins dissociate. Translocation

Abbreviations: AP-1, activating protein 1; CD, circular dichroism; CHAPS, 3-[(3-cholamidopropyl)dimethylammonio]-1-propanesulfonate; DEX, Dexamethasone; DTT, dithiothreitol; EDTA, ethylenediaminetetraacetic acid; FP, fluorescence polarization; GPCR, G-protein coupled receptor; GR, glucocorticoid receptor; GRE, glucocorticoid response element; HEPES, 4-(2-hydroxyethyl)-1-piperasineethanesulfonic acid; HSP90, heat shock protein 90; ITC, isothermal titration calorimetry; LBD, ligand binding domain; LGICR, ligand-gated ion channel receptors; NCoR, nuclear receptor corepressor; NF-κB, nuclear factor kappa B; PMSF, phenylmethanesulfonyl fluoride; SEC-MS, size-exclusion chromatography mass spectrometry; SPR, Surface Plasmon Resonance; TAMRA, carboxytetramethylrhodamine; TCEP, tris(2-carboxyethyl) phosphine hydrochloride; TIF2, transcriptional intermediary factor 2.

* Corresponding author. Tel.: +1 203 798 5129; fax: +1 203 791 6196.
E-mail address: mlabadia@rdg.boehringer-ingelheim.com (M.E. Labadia).

0301-4622/$ - see front matter © 2007 Elsevier B.V. All rights reserved.
doi:10.1016/j.bpc.2007.03.013

of GR into the nucleus follows this dissociation. Once inside the nucleus, GR regulates transcription either through direct interactions with the promoter region of target genes or through interactions with transcriptional factors such as NF-κB and AP-1.

GR can bind to either positive or negative glucocorticoid response elements (GREs) in the nucleus. *Cis*-activation through positive GREs occurs when either GR homo or heterodimers bind to the palindromic consensus sequence GGTACAnnnTGTTCT [1]. *Cis*-repression by GR occurs through an interaction with a negative GRE half site. *Trans*-repression can occur through the direct interaction between GR and transcription factors. Current models of inflammation suggest that *trans*-repression of transcription factors is the primary mechanism by which GR ligands mediate their anti-inflammatory activity. In contrast it is thought that the side effects of GR ligands are primarily mediated through either *cis*-activation or *cis*-repression of gene expression. Current theories postulate that differential recruitment of co-factors to targeted DNA promoter regions by GR may be the underlying mechanism determining selectivity between anti-inflammatory and side effect pathways [2].

GR consists of three main functional domains. The N-terminal region contains a non-ligand-dependent activation domain which is associated with turning on gene expression once GR is bound to DNA. The central region of the GR molecule contains the DNA binding domain which consists of two zinc fingers. The C-terminal region of GR contains the ligand binding domain (LBD). A second activation domain lies within the LBD and is thought to be associated with ligand-dependent regulation of gene expression [3].

The crystal structure of GR-LBD(F602S) in complex with Dexamethasone (DEX) and a peptide derived from coactivating co-factor transcriptional intermediary factor 2 (TIF2) has been solved by Bledsoe et al. [4]. This structure reveals that, when agonist (DEX) is bound to GR-LBD(F602S), two charge clamps mediate the selectivity for TIF2 recognition by GR. The crystal structure of GR-LBD(F602S) in complex with the antagonist RU-486 shows a large conformational change in helix 12 [5] that has been postulated to block the ability to bind coactivator. Co-immunoprecipitation studies with GR and the corepressor NCoR show that when RU-486 is bound, NCoR interacts with both the N and C-terminus of full length GR [6]. Consistent with the structural data, MS-based deuterium exchange measurements suggest that RU-486 binding provokes the unfolding of helix 12. These measurements also imply that the binding sites for TIF2 and NCoR are largely overlapping. Here we further describe how distinct co-factors bind to a similar or overlapping GR-LBD (F602S) pocket via differences in thermodynamic recognition.

2. Experimental procedures

2.1. Peptides

Both TIF2 and NCoR peptides were obtained from AnaSpec Inc. The TIF2 sequence used was KENALLRYLLDKDD while the NCoR-ID2 sequence was ASNLGLEDIIRKALMGSFD [8]. The same TIF2 peptide was obtained from AnaSpec Inc. with a TAMRA fluorophore directly linked to the N-terminus.

2.2. Protein expression and purification

The GR-LBD(F602S) was expressed as a glutathione-*S*-transferase (GST) fusion protein in *Escherichia coli* BL21 (DE3) cells [4]. Cells were grown at 37 °C in LB medium to an OD_{600} of 0.8. The temperature was then reduced to 15 °C. Once the cells attained an OD_{600} of 1.0, protein expression was induced with 30 μM isopropyl-β-D-galactoside and 200 μM Dexamethasone was added to the Media. The cells were harvested 15 h post induction and frozen at −80 °C.

Cells were thawed and mixed with 4 °C lysis buffer (50 mM Tris–HCl, pH 8.0, 150 mM KCl, 10% Glycerol, 0.5 mM EDTA, 10 mM DTT, 1 mM PMSF, 4 μg/mL Pepstatin A, 4 μg/mL Leupeptin, 0.04% CHAPS, 2 M Urea and 50 μM Dexamethasone) at a ratio of 5 mL/g of cells. The cells were homogenized on ice using a PolyTron PT 2100 (Kinematica AG, Switzerland) then sonicated with a Branson Sonifier 450 (Converter, USA). The cell lysate was centrifuged at 44,000 rpm for 60 min at 4 °C.

Using an AKTA Prime chromatography system (Amersham, Sweden) the clarified lysate was purified by affinity chromatography on Glutathione Sepharose 4B resin (GS4B) (Amersham, Sweden). While the protein was bound to the resin the urea was removed with a linear gradient of 4 °C wash buffer (50 mM Tris–HCl, pH 8.0, 150 mM KCl, 10% Glycerol, 0.5 mM EDTA, 10 mM DTT, 0.1% CHAPS and 50 μM Dexamethasone). The GR-LBD(F602S) was cleaved from the GST-tag by incubating the resin overnight at 4 °C with thrombin protease (USB, USA) in the presence of 2.5 mM $CaCl_2$. The thrombin flow through was collected and dialyzed into 4 °C IEX buffer A (10 mM Tris–HCl, pH 7.8, 10% Glycerol, 0.5% CHAPS, 1 mM DTT and 50 μM Dexamethasone). The GR-LBD(F602S) was further purified by anion exchange chromatography on Micro Prep 25 Q resin (BioRad, Ca). The 25 Q resin was eluted using a linear gradient with 4 °C IEX buffer B (1 M NaCl and IEX buffer A). The GR-LBD(F602S) was dialyzed at 4 °C into a storage buffer (20 mM HEPES, pH 7.4, 200 mM NaCl, 10% Glycerol, 0.04% CHAPS, 1 mM DTT and 35 μM Dexamethasone). The final product, GR-LBD(F602S) contains 258 residues and has a molecular weight of 29,798 g/mol.

2.3. Ligand exchange

Purified GR-LBD(F602S) was diluted to 10 μM in a pH 7.4 buffer containing 20 mM HEPES, 200 mM NaCl, 1 mM TCEP and either 10 μM Dexamethasone or 10 μM RU-486. The samples were exhaustively dialyzed to ensure complete exchange of ligand. Ligand exchange was confirmed by SEC-MS where the percentages of DEX, RU-486 both bound to GR-LBD(F602S) and free in solution were quantified. After dialysis GR-LBD (F602S) was concentrated in a Vivaspin 10,000 MWCO PES concentrator (Vivascience, Germany). The final protein concentration was determined using a Biorad DC Protein Assay.

2.4. Confirmation of ligand exchange

Ligand exchange was confirmed using size exclusion chromatography–mass spectrometry (SEC-MS). This method was

used to quantify the percentages of DEX and RU-486 both bound to GR-LBD (F602S) and free in solution. The apparatus used for ligand exchange confirmation is a modification of that used by Blom et al. consisting of an Agilent HPLC with a G1313A automatic liquid sampler and G1311A quaternary pump (Agilent Technologies, USA) [9]. A BioSep-SEC-S3000 SEC column, 30×2 mm (Phenomenex, Ca.) was equilibrated with a pH 7.4 buffer containing 20 mM HEPES, 100 mM NaCl and 1 mM TCEP. 10 μL samples were injected onto the column at a flow rate of 0.4 mL/min. The SEC column was used to quickly (<30 s) separate GR-LBD(F602S) and GR-LBD(F602S)-ligand complex from ligand free in solution. The GR-LBD(F602S)-ligand complex was directed to a Protein Micro Trap, 1×8 mm (Michrom BioResources, Inc., Ca.) while a LabPro automatic valve (Rheodyne, Ca.) diverted retained components (smaller than 3000 Da) to waste. The Micro Trap was flushed for 1.5 min with water at a flow rate of 0.4 mL/min from a Kratos Spectroflow solvent delivery system (Kratos, USA) to remove salt and buffer. A second LabPro valve directs the flow of a Shimadzu HPLC consisting of two LC-10AD pumps and an SLC-10A system Controller (Shimadzu Scientific Instruments, Md.) to the Micro Trap in the reverse direction. At this point a mobile phase is delivered at a flow rate of 0.25 mL/min to the Micro trap consisting of water with 5% acetonitrile and 0.1% formic acid at a flow of 0.25 mL/min. GR-LBD(F602S) is denatured by the low pH of the mobile phase and bound DEX and/or RU-486 are released. An acetonitrile gradient from 5% to 95% transfers the denatured sample to a Luna C18(2) MercuryMS column, 20×2 mm (Phenomenex, Ca.) for separation of GR-LBD (F602S) and released DEX and/or RU-486. The column effluent is directed to a Qtof API US mass spectrometer (Water Corporation, Ma.) operated in positive electrospray mode (1 s scans from $m/z=50$ to 900 are collected and stored). Responses for DEX ($m/z=393.2077$ (1+)) and RU-486 ($m/z=430.2746$(1+)) are extracted for each injection. A third LabPro valve added between the auto-sampler and SEC column permitted injection of standard solutions of DEX and RU-486 to be directed to the Micro Trap for quantification, bypassing the SEC column. This also is used to direct sample injections to the Micro Trap for quantification of total DEX and/or RU-486 both bound to GR-LBD (F602S) and in solution.

2.5. Analytical ultracentrifugation

All experiments were conducted on a Beckman XL-I analytical ultracentrifuge. All sedimentation velocity experiments were conducted at 50,000 rpm and 20 °C. Experiments on GR-LBD(F602S) were conducted in a pH 7.4 buffer containing 20 mM HEPES, 200 mM NaCl, 1 mM TCEP and either 10 μM Dexamethasone or RU-486. Data were collected at either 230 or 280 nm and were analyzed using SedFit version 8.9 [10]. Sedimentation coefficients were calculated using a solvent density of $\rho=1.00704$ g/mL and a viscosity of 1.0259 cp. The partial specific volume for GR-LBD(F602S) ($\upsilon=0.7433$ mL/g) was calculated from the amino acid sequence using the software program Sednterp version 1.07.

Sedimentation equilibrium experiments were carried out at 20 °C. Equilibrium data for three concentrations were collected at 280 nm at 17,500, 20,000, 22,500, and 25,000 rpm. Data were analyzed using WINnonlin version 1.07. Molecular weights were calculated from σ using the calculated solvent density, viscosity and a partial specific volume as listed above. All analytical ultracentrifugation software listed above is available online at http://www.bbri.org/RASMB/rasmb.html.

2.6. Solution competition binding — Surface Plasmon Resonance (SPR)

All SPR experiments were performed on a BIAcore 3000™ instrument at 25 °C in the following buffer: 20 mM HEPES, pH 7.4, 200 mM NaCl, 500 μM TCEP, 0.04% CHAPS and 0.5% DMSO. SPR binding surfaces were prepared by immobilizing approximately 300–400 RU of biotinylated coactivator (TIF2) or corepressor (NCoR-ID2) peptides on NeutrAvidin charged CM4 chips. Solution competition experiments were performed by incubating a range of TIF2 or NCoR-ID2 peptide concentrations with 200 nM GR-LBD(F602S) bound with Dexamethasone or RU-486. These reaction mixtures were then injected over immobilized TIF2 and NCoR-ID2 surfaces at a flow rate of 30 μL/min until equilibrium was reached. Equilibrium data were analyzed using BIAevaluation software (BIAcore) and the solution IC_{50}'s were estimated by non-linear regression analysis using the Marquardt–Levenburg minimization method (SAS version 8.0).

2.7. Circular dichroism

Far-UV circular dichroism spectra for GR-LBD(F602S) bound with either Dexamethasone or RU-486 were collected at room temperature in a pH 7.4 buffer containing 20 mM HEPES, 200 mM NaCl, 1 mM TCEP and either 10 μM Dexamethasone or RU-486 using a Jasco J-720 spectropolarimeter. Spectra were collected from 260–180 nm in 0.01 cm path length quartz cuvettes at a scanning speed of 100 nm/min, a data pitch of 0.1 nm and an accumulation of 10. Buffer blanks were collected under the same conditions and subtracted from the data. The raw circular dichroism signals were converted to mean residue ellipticity using the following equation $\theta_{mrd}=\theta_d*(M/cln_r)$ where θ_d is the ellipticity measured in degrees, M is the molecular weight measured in g/dmol, c is the concentration measured as g/cm^3, l is the path length measured in cm and n is the number of amino acid residues. The mean residue ellipticity for both GR-LBD (F602S) bound with Dexamethasone and RU-486 were fit from 260 to 190 nm using the software package CDPro (http://lamar.colostate.edu/~sreeram/CDPro/) which allows the user to compare secondary structure calculations from three different CD programs (SELCON3, CDSSTR and CONTIN).

2.8. Isothermal titration calorimetry (ITC)

The isothermal titration calorimetry experiments were performed using a Microcal VP-ITC from Microcal, Inc.

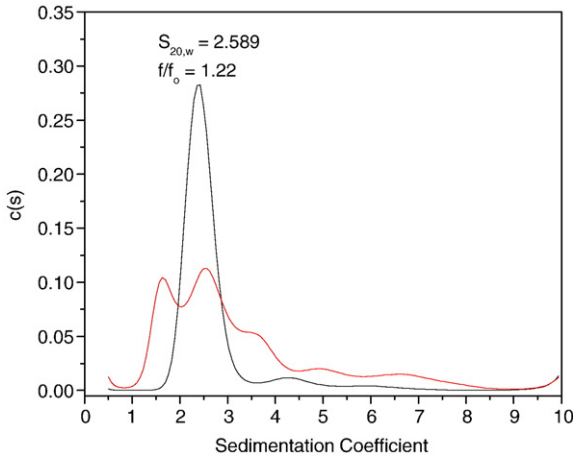

Fig. 1. Sedimentation velocity data collected at 280 nm for 8.6 μM GR-LBD (F602S) showing that GR-LBD(F602S) is a monomer under physiological conditions when Dexamethasone is present (black). Removal of Dexamethasone results in the slow unfolding and aggregation of 2 μM GR-LBD(F602S) (red) as monitored at 230 nm. (For interpretation of the references to colour in this figure legend, the reader is referred to the web version of this article.)

Table 1
K_d's for TIF2 and NCoR-ID2 binding to GR-LBD(F602S)/DEX and GR-LBD (F602S)/RU-486 as determined by both fluorescence polarization (FP) and Surface Plasmon Resonance

	TIF2		NCoR-ID2
Compound	FP K_d (μM)	BIAcore IC_{50} (μM)	BIAcore IC_{50} (μM)
DEX	1.9±0.2	3.1±0.7 (K_d)	>150
RU-486	>20[a]	>200	14±4

[a] These data were fit by fixing the plateau value for the curve.

(Northampton, MA). The sample cell of the calorimeter was loaded with GR-LBD(F602S) bound with either Dexamethasone or RU-486 in a pH 7.4 buffer containing 20 mM HEPES, 150 mM NaCl, 1 mM TCEP and either 10 μM Dexamethasone or RU-486. The syringe was loaded with TIF2 or NCoR-ID2 peptide for GR-LBD(F602S)/DEX and GR-LBD(F602S)/RU-486 respectively dissolved in the same buffer. All solutions were degassed for 8 min. Titrations were performed at 25 °C with an injection volume of 10 μL and spacing of 500 s. After completion of the titration, baselines were manually drawn and subtracted from the data. The data were zeroed assuming that the final injections of each titration

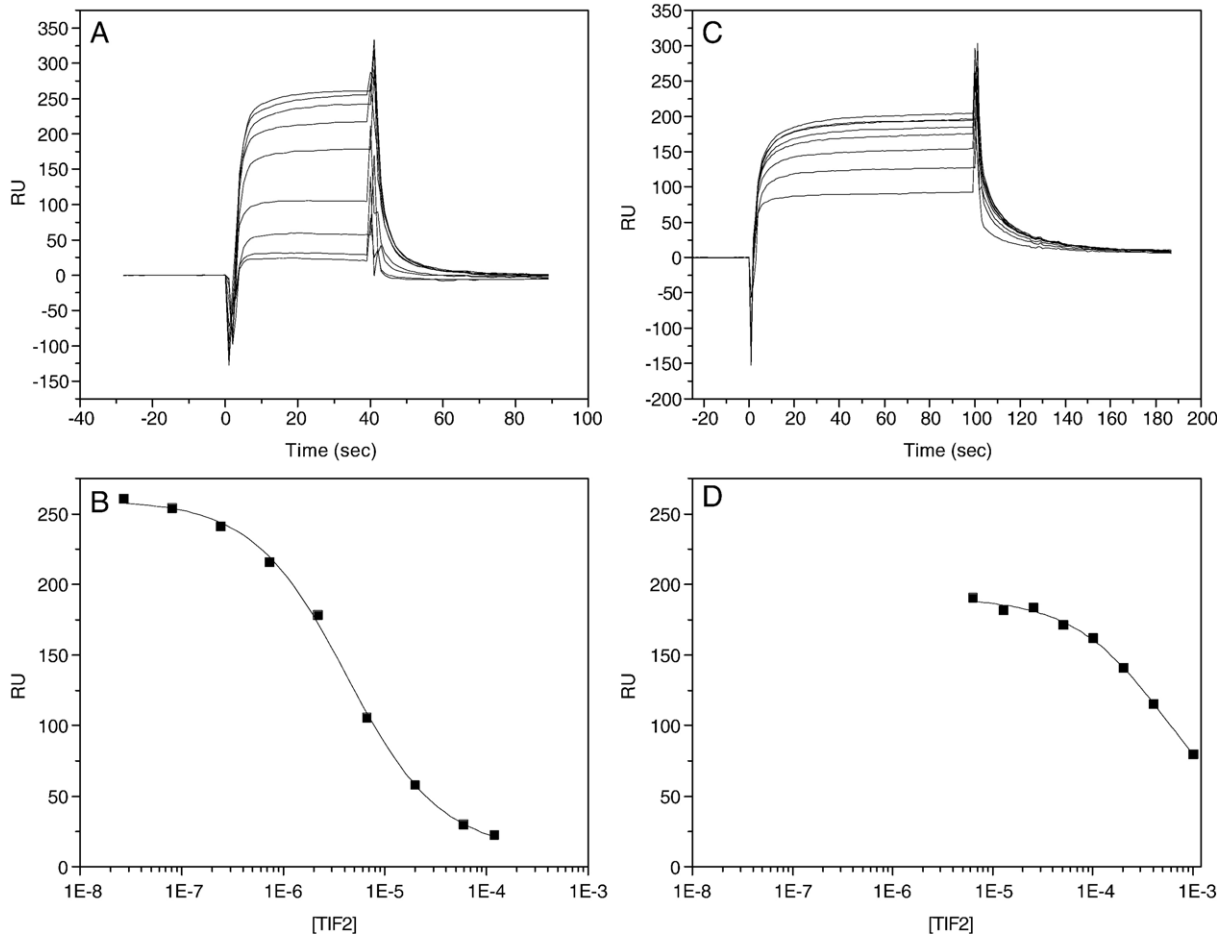

Fig. 2. Surface Plasmon Resonance of GR-LBD(F602S)/DEX (A and B) titrated with TIF2 from 27 nM to 120 μM and GR-LBD(F602S)/RU-486 (C and D) titrated with TIF2 from 6.25 μM to 1 mM. Top panel graphs show raw SPR data. Data points plotted in the bottom panel graphs depict the equilibrium response units for each concentration of GR-LBD(F602S) injected over the surface.

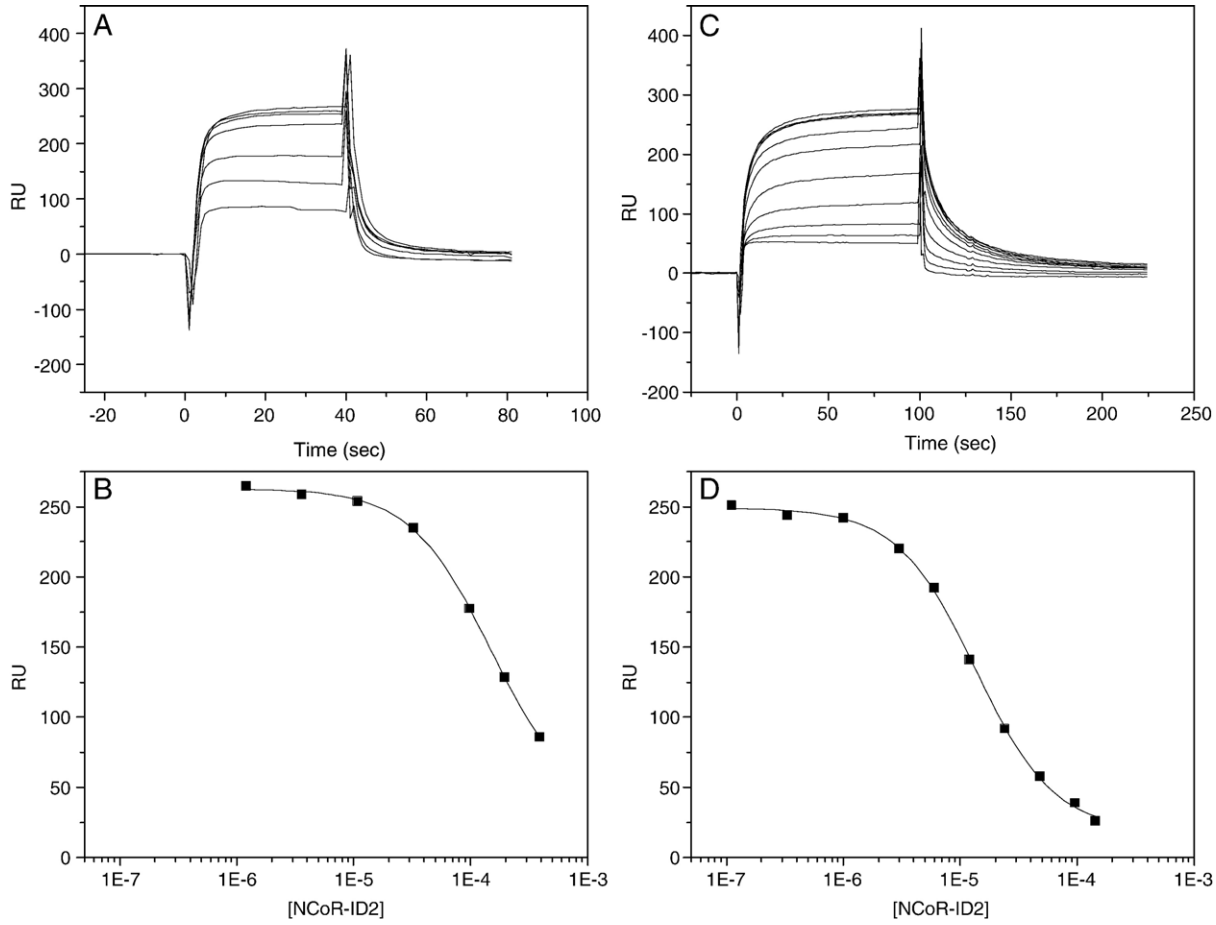

Fig. 3. Surface Plasmon Resonance of GR-LBD(F602S)/DEX (A and B) titrated with NCoR-ID2 from 1.2 μM to 390 μM and GR-LBD(F602S)/RU-486 (C and D) titrated with NCoR-ID2 from 111 nM to 144 μM. Top panel graphs show raw SPR data. Data points plotted in the bottom panel graphs depict the equilibrium response units for each concentration of GR-LBD(F602S) injected over the surface.

represent only the heat of dilution. Data were fit using a one-site binding model available in the Origin ITC data analysis software (version 5.0).

2.9. Fluorescence polarization (FP)

All fluorescence polarization binding titrations were performed at room temperature in a pH 7.4 buffer containing 20 mM HEPES, 200 mM NaCl, 1 mM TCEP, 0.04% CHAPS and either 10 μM Dexamethasone or RU-486, in Corning 96 well half-area flat bottom non-binding surface plates. Each experiment contained 25 nM of the fluorescently labeled TIF2 peptide with increasing amounts of either GR-LBD(F602S)/DEX or GR-LBD(F602S)/RU-486. All FP measurements were made on an LJL Biosystems Analyst AD System 96/384 well plate reader with a 550 nm (20) filter in the excitation path, a 580 nm (10) filter in the emission path and a rhodamine 561 dichroic mirror. A well containing 25 nM fluorescently labeled TIF2 was included to allow determination of the free probe polarization. Data were fit using a single binding site model via nonlinear least squares regression analysis. The analysis algorithm includes correction for protein binding-induced changes in the fluorescence intensity of the fluorophore.

3. Results

Prior to performing binding experiments, GR-LBD(F602S) and GR-LBD(F602S) bound with Dexamethasone were analyzed by sedimentation velocity. The data in Fig. 1 show the $c(s)$ distribution for both conditions. These data show that when GR-LBD(F602S) is bound with Dexamethasone it is primarily monomer with a small amount of dimer. The concentration of GR-LBD(F602S) in this experiment is 8.3 μM. Some higher order aggregated species can also be detected under these conditions. When Dexamethasone is not bound the GR-LBD(F602S) unfolds and aggregates as shown by the red curve in Fig. 1. These results are not in agreement with data published by Bledsoe et al. who report a K_d for

Table 2
Sedimentation velocity data of GR-LBD(F602S)/DEX and GR-LBD(F602S)/RU-486 with and without TIF2 and NCoR-ID2

Components	$S_{20,w}$	f/f_0
GR-LBD(F602S)/DEX	2.589 [2.563,2.609]	1.22
GR-LBD(F602S)/DEX+TIF2	2.676 [2.650,2.708]	1.27
GR-LBD(F602S)/RU-486	2.598 [2.586,2.604]	1.26
GR-LBD(F602S)/RU-486+NCoR-ID2	2.687 [2.682,2.694]	1.26

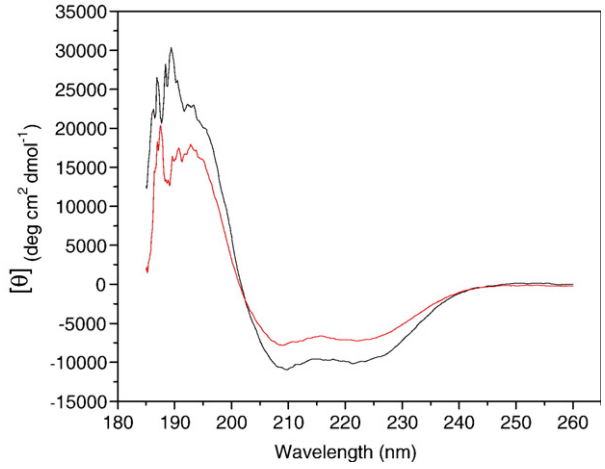

Fig. 4. Circular dichroism spectra of GR-LBD(F602S)/DEX (black) and GR-LBD(F602S)/RU-486 (red). (For interpretation of the references to colour in this figure legend, the reader is referred to the web version of this article.)

dimerization of GR-LBD(F602S) of 1.5 μM [4]. To further investigate this discrepancy a sedimentation equilibrium experiment was performed to measure the K_d for GR-LBD (F602S) dimerization in the presence of Dexamethasone. Global analysis of the sedimentation equilibrium data show that GR-LBD(F602S) is primarily monomeric (data not shown). Data analysis of the sedimentation equilibrium data including a dimer species fits to a dimerization K_d=13 μM. However, including dimer in the model does not statistically improve the quality of the fit. To explain the earlier data published by Bledsoe et al., the buffer conditions were duplicated and velocity and equilibrium experiments were performed. It was observed that in the absence of reducing agent GR-LBD(F602S) aggregates. It is likely that the apparent dimerization K_d measured by Bledsoe et al. was influenced by aggregating GR-LBD(F602S) formed via inter-molecular di-sulfide bonding.

To determine co-factor affinity and selectivity of GR-LBD (F602S) when bound with agonist versus antagonist, fluorescence polarization and solution competition SPR experiments were performed with GR-LBD(F602S) bound to either Dexamethasone or the antagonist RU-486. Co-factor affinity and selectivity were determined for the coactivator peptide TIF2 and the corepressor peptide NCoR-ID2. Shown in Fig. 2 is a representative experiment for TIF-2 binding to GR-LBD(F602S) bound with DEX or RU-486. The K_d for TIF-2 binding GR-LBD (F602S)/DEX was determined to be 3.1 μM. This measurement is in good agreement with the affinity constant determined by fluorescence polarization (FP) (Table 1). In contrast, TIF-2 bound weakly (>200 μM by SPR, >20 μM by FP) to GR-LBD(F602S) bound with the antagonist RU-486 (Fig. 2. C, D, Table 1). The reverse specificity was observed for the corepressor peptide NCoR-ID2 binding to GR-LBD(F602S) bound with antagonist. NCoR-ID2 bound GR-LBD(F602S)/RU-486 with an IC_{50} of

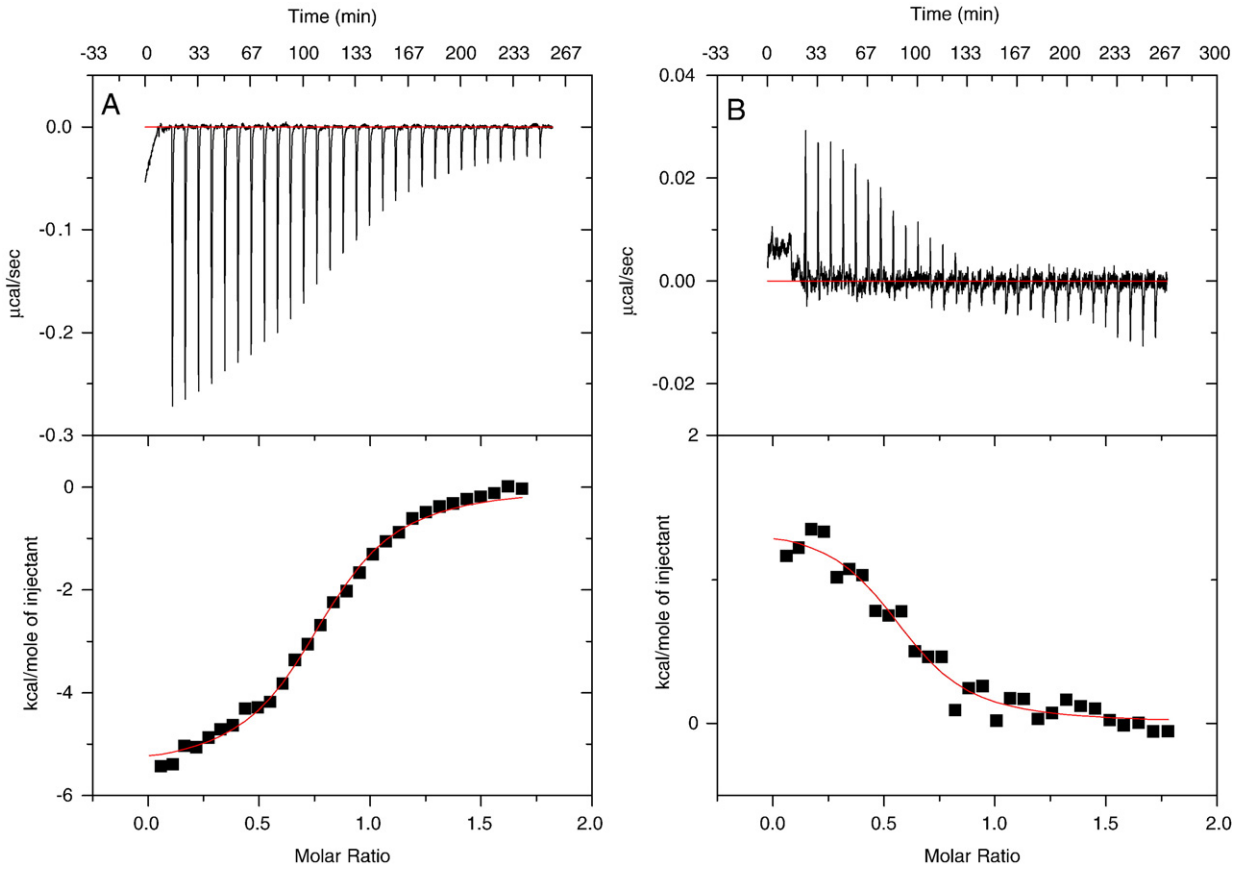

Fig. 5. Isothermal titration calorimetry of (A) 150 μM TIF2 titrated into 20 μM GR-LBD(F602S)/DEX at 25 °C, (B) 95 μM NCoR-ID2 titrated into 12 μM GR-LBD (F602S)/RU-486 at 25 °C.

Table 3
Thermodynamic data for GR-LBD(F602S)/DEX binding TIF2 and GR-LBD(F602S)/RU-486 binding NCoR-ID2 at 25 °C

Components	K_d (μM)[a]	ΔH_{app} (kcal/mol)	$T\Delta S_{app}$ (kcal/mol)
GR-LBD(F602S)/DEX+TIF2 @ 25 °C	0.9±0.1	−5.5±0.08	2.8
GR-LBD(F602S)/PRED+TIF2 @ 25 °C	0.8±0.1	−6.6±0.2	1.7
GR-LBD(F602S)/FLU+TIF2 @ 25 °C	0.5±0.08	−6.6±0.2	2.0
GR-LBD(F602S)/RU-486+NCoR-ID2 @ 25 °C	0.6±0.2	1.4±0.08	9.9

[a] The data presented in these table are each the result of a single titration.

14 μM and an IC_{50} of >150 μM when bound to GR-LBD(F602S)/DEX (Fig. 3 and Table 1). The observation that TIF-2 can compete for GR-LBD(F602S) binding to immobilized NCoR-ID2 and vice versa, albeit with weak affinity, support the findings by Frego et al. that TIF-2 and NCoR recognize the same or overlapping binding pocket on GR-LBD [7]. However, co-factor binding affinity and subsequent selectivity is dictated by conformations induced by bound agonist or antagonist.

Sedimentation velocity experiments of GR-LBD(F602S) bound either with Dexamethasone or RU-486 in the presence and absence of co-effector peptide were conducted to determine if co-factor binding influences the association state of GR-LBD (F602S). Under all of the conditions tested GR-LBD(F602S) remains monomeric when co-effector peptide binds (Table 2). This supports the validity of fitting the SPR and fluorescence data with a simple 1:1 binding model. The small increases observed in the sedimentation coefficient when co-factor binds to GR-LBD(F602S) are consistent with the increase in mass of the co-complex, however, the shifts are small and these experiments were not repeated enough times to draw this conclusion definitively. Also listed in Table 2 are the fit f/f_0 values for each complex. The f/f_0 ratio provides an estimate of the weight-average frictional coefficient of GR-LBD under each condition. The f/f_0 values suggest that large shape changes are not occurring when co-factor binds to GR-LBD(F602).

Far-UV circular dichroism spectra were collected for GR-LBD(F602S) bound with either Dexamethasone or RU-486. The CD spectra show the loss of α-helix, monitored at 222 nm, that occurs when RU-486 binds (Fig. 4). The unfolding of helix 12 has been shown previously in the published crystal structure of this complex and also by deuterium mass spectrometry studies [5,7].

Fig. 5 shows isothermal titration calorimetry data for coactivator peptide TIF2 binding to GR-LBD(F602S)/DEX and corepressor peptide NCoR-ID2 binding to GR-LBD (F602S)/RU-486. The binding thermodynamics for each of these interactions are shown in Table 3. The binding interaction between TIF2 and GR-LBD(F602S)/DEX is driven by both favorable enthalpic and entropic interactions whereas the interaction between NCoR-ID2 and GR-LBD(F602S)/RU-486 is primarily entropically driven. This is an intriguing result given that it has been shown by Frego et al. that both peptides utilize the same binding pocket on GR-LBD(F602S) [7]. These data show that while binding to the same pocket the amino acids recognized in the binding pocket are likely different for each peptide. It should be noted, that the enthalpy and entropy changes reported in Table 3 are apparent values observed in a specific buffer at a single temperature. From these data the role of protonation in the recognition of TIF2 and NCoR binding to GRLBD(F602S) cannot be evaluated. Ideally multiple temperatures and buffer systems would be examined but difficulty in obtaining the quantity of stably exchanged material prevented exhaustive analysis.

Isothermal titration calorimetry (ITC) experiments were also conducted with GR-LBD(F602S) bound with the agonists Prednisolone (PRED) and Fluticasone (FLU) (Table 3). These data show similar apparent changes in enthalpy and entropy as compared to DEX. GR-LBD(F602S) bound with either Prednisolone or Fluticasone were observed to selectively bind TIF2 over NCoR-ID2 (Biacore data not shown). These data provide additional evidence that bound ligand dictates whether coactivator or corepressor binds to GR.

4. Discussion

The study described herein was designed to determine the affinity and thermodynamic properties of agonist and/or antagonist bound GR-LBD (F602S) binding to the coactivator peptide TIF-2 and the corepressor peptide NCoR-ID2. The co-factors chosen for these studies were selected specifically to address areas of GR regulation where it would be beneficial to either suppress or enhance function. Through interaction with coactivators, nuclear hormone receptors recruit histone acetyl transferases to specific DNA promoter regions. This ultimately results in transcriptional activation [11]. TIF2 includes several repeats of the motif (LXXLL) that has been shown to interact with nuclear receptor proteins. The TIF2 peptide used herein includes the central portion of the third repeat, which was shown by Ding et al. to be preferred by GR [12]. It also includes the portion of the TIF2 peptide used to generate the GR-LBD(F602S)/DEX/TIF2 crystal structure described in Bledsoe et al. [4]. In contrast to the effect of coactivators, the interaction of corepressors with nuclear hormone receptors results in the repression of transcription through recruitment of histone deacetylases [13]. These interactions have been shown to occur with nuclear hormone receptors in the unliganded state, although antagonists have been reported to stabilize the interaction [14]. The corepressor peptide (NCoR-ID2) used in the studies presented here is a portion of the CoRNR box, which has been shown to be required for interaction with nuclear hormone receptors [8], and contains the L/I-X-X-I/V-I conserved motif.

These studies show that neither Dexamethasone nor RU-486 has an effect on the oligomeric state of GR-LBD(F602S). Our data show that previously published reports of GR-LBD solution dimerization in the low micromolar range are likely due to aggregation mediated via di-sulfide linkage. The GR-LBD

(F602S) construct is highly unstable in the absence of bound ligand. In addition we have observed that GR-LBD(F602S) bound with RU-486 is less stable than GR-LBD(F602S) bound with Dexamethasone. This is likely the result of the un-folding of helix 12 that occurs when antagonist binds. Due to the unstable nature of the GR-LBD(F602S) construct efforts were made to ensure high quality protein was used in all of the biophysical analyses by performing analytical ultracentrifugation and mass-spectrometry confirming presence of bound ligand prior to all experimental studies.

Recent studies have proposed a coactivator/corepressor equilibrium model for GR-mediated activation or repression of gene transcription. The model states that agonist or antagonist bound GR can bind coactivators as well as corepressors and the ratio of the two populations dictates transcriptional regulation [14,15]. In support of this model, mammalian two-hybrid assays have demonstrated that both the coactivator TIF2 and the corepressor NCoR-RID can interact with GR bound with agonist or antagonist [15]. However, the data clearly show that GR-DEX prefers TIF2 and GR-RU486 prefers NCoR-RID. These results are consistent with the co-factor selectivity determined by SPR and FP affinity measurements for GR-LBD(F602S) bound with agonist or antagonist presented here. In contrast to our data, the mammalian two-hybrid assay system was unable to detect an interaction between GR-LBD and NCoR-ID2 in the presence of either agonist or antagonist suggesting that both the amino- and carboxyl-terminal regions of GR are required for binding to NCoR-ID2. The data presented here demonstrate that GR-LBD(F602S) bound with RU486 binds NcoR-ID2 which is consistent with studies by Hu and Lazar [8]. This may be due to an increased sensitivity of the biophysical methods employed in the studies presented here relative to mammalian two-hybrid and co-immunoprecipitation assays for the detection of these interactions. Our data demonstrate that the LBD of GR when bound with agonist or antagonist displays co-factor selectivity similar to full-length GR.

Based on studies conducted here with GR-LBD(F602S) it is the ligand that dictates the conformational change in GR resulting in differential co-factor binding. This hypothesis is further supported by previous reports demonstrating that the partial agonist activity of antagonist-occupied steroid receptors is regulated by conformational-induced recruitment of a novel coactivator protein that recognizes the hinge region of PR [14]. It has been shown previously that both activating and repressing co-factors utilize a similar or overlapping binding pocket on GR-LBD(F602S) [7]. Here we show that the binding affinities for both a coactivator and corepressor peptide are similar yet the affinity is achieved via different thermodynamic mechanisms. Binding of coactivator to GRLBD(F602S) is driven by both favorable enthalpic and entropic interactions. The favorable enthalpic interactions likely derive from the interaction between the two charge clamps formed between GRLBD(F602S) residues (E755, K579, D590, R585) and the coactivator peptide. In contrast, the binding of corepressor to GRLBD(F602S) is driven primarily by favorable entropic interactions. After antagonist binds the unfolding of helix 12 results in movement of the charge clamp residues away from the co-effector binding pocket. The resulting exposed solvent accessible surface area is significantly less polar than when agonist is bound. This change in polarity of the co-effector binding pocket allows thermodynamic discrimination of co-effector binding. Similar thermodynamic studies have been conducted examining the thermodynamic discrimination of agonist versus antagonist binding to G-protein coupled receptors (GPCRs) as well as ligand-gated ion channel receptors (LGICRs) [16]. These studies suggest that the thermodynamic mechanism by which a ligand binds could be predictive of its agonistic versus antagonistic activity for certain receptors.

Hydrogen–deuterium exchange experiments conducted with GPCRs and LGICRs have shown, similar to the glucocorticoid receptor, that agonist and antagonist ligands induce changes in structure that are often linked to the thermodynamic discrimination of the ligands [17]. Our studies take the analysis of ligand-induced structural changes one step further. While we do not know if agonist versus antagonist binding to GR is thermodynamically discriminated our data suggests that discrimination does exist for coactivator versus corepressor proteins. It remains to be tested whether this theme holds true for additional coactivator and corepressor proteins binding to GR.

Acknowledgements

The authors are indebted to the following individuals for their contributions to this work: Dr. Joey Studts for advice during expression trials. Alistair Baptiste for completing large scale *E. coli* fermentations using optimized expression parameters.

References

[1] A. Dostert, T. Heinzel, Negative glucocorticoid receptor response elements and their role in glucocorticoid action, Curr. Pharm. Des. 10 (2004) 2807–2816.
[2] M.J. Coghlan, P.B. Jacobson, B. Lane, M. Nakane, C.W. Lin, S.W. Elmore, P.R. Kym, J.R. Luly, G.W. Carter, R. Turner, C.M. Tyree, J. Hu, J.R. Elgort, J.N. Miner, A novel anti-inflammatory maintains glucocorticoid efficacy with reduced side effects, Mol. Endocrinol. 17 (2003) 860–869.
[3] I.M. Adcock, Molecular mechanisms of glucocorticoid actions, Pulm. Pharmacol. Ther. 13 (2000) 115–126.
[4] R.K. Bledsoe, V.G. Montana, T.B. Stanley, C.J. Delves, C.J. Apolito, D.D. McKee, T.G. Consler, D.J. Parks, E.L. Stewart, T.M. Willson, M.H. Lambert, J.T. Moore, K.H. Pearce, H.E. Xu, Crystal structure of the glucocorticoid receptor ligand binding domain reveals a novel mode of receptor dimerization and coactivator recognition, Cell 110 (2002) 93–105.
[5] B. Kauppi, C. Jakob, M. Farnegardh, J. Yang, H. Ahola, M. Alarcon, K. Calles, O. Engstrom, J. Harlan, S. Muchmore, A.K. Ramqvist, S. Thorell, L. Ohman, J. Greer, J.A. Gustafsson, J. Carlstedt-Duke, M. Carlquist, The three dimensional structures of antagonistic and agonistic forms of the glucocorticoid receptor ligand-binding domain, J. Biol. Chem. 278 (2003) 22748–22754.
[6] M. Schulz, M. Eggert, A. Baniahmad, A. Dostert, T. Heinzel, R. Renkawitz, RU486-induced glucocorticoid receptor agonism is controlled by the receptor N terminus and by corepressor binding, J. Biol. Chem. 277 (2002) 26238–26243.
[7] L. Frego, W. Davidson, Conformational changes of the glucocorticoid receptor ligand binding domain induced by ligand and cofactor binding, and the location of cofactor binding sites determined by hydrogen/deuterium exchange mass spectrometry, Protein Sci. 15 (2006) 722–730.

[8] X. Hu, M.A. Lazar, The CoRNR motif controls the recruitment of corepressors by nuclear hormone receptors, Nature 402 (1999) 93–96.
[9] K.F. Blom, B.S. Larsen, C.N. McEwen, Determining affinity-selected ligands and estimating binding affinities by online size exclusion chromatography/liquid chromatography–mass spectrometry, J. Com. Chem. 1 (1999) 82–90.
[10] P. Schuck, Size distribution analysis of macromolecules by sedimentation velocity ultracentrifugation and Lamm equation modeling, Biophys. J. 78 (2000) 1606–1619.
[11] J. Xu, Q. Li, Review of the in vivo functions of the p160 steroid receptor coactivator family, Mol. Endocrinol. 17 (2003) 1681–1692.
[12] X.F. Ding, C.M. Anderson, H. Ma, H. Hong, R.M. Uht, P.J. Kushner, M.R. Stallcup, Nuclear receptor-binding sites of coactivators glucocorticoid receptor interacting protein 1 (GRIP1) and steroid-receptor coactivator 1 (SRC-1): multiple motifs with different binding specificities, Mol. Endocrinol. 12 (2) (1998) 302–313.
[13] H.E. Xu, T.B. Stanley, V.G. Montana, M.H. Lambert, B.G. Shearer, J.E. Cobb, D.D. McKee, C.M. Galardi, K.D. Plunket, R.T. Nolte, D.J. Parks, J.T. Moore, S.A. Kliewer, T.M. Willson, J.B. Stimmel, Structural basis for antagonist-mediated recruitment of nuclear co-repressors by PPARalpha, Nature 415 (2002) 813–817.
[14] A.T. Jackson, J.K. Richer, D.L. Bain, G.S. Takimoto, L. Tung, K.B. Horwitz, The partial agonist activity of antagonist-occupied steroid receptors is controlled by a novel hinge domain-binding coactivator L7/SPA and the corepressors N0CoR or SMRT, Mol. Endocrinol. 11 (6) (1997) 693–705.
[15] Q. Wang, J.A. Blackford Jr., L.N. Song, Y. Huang, S. Cho, S.S. Simons Jr., Equilibrium interactions of corepressors and coactivators with agonist and antagonist complexes of glucocorticoid receptors, Mol. Endocrinol. 18 (2004) 1376–1395.
[16] P.A. Borea, A. Dalpiaz, K. Varani, P. Gilli, G. Gilli, Can thermodynamic measurements of receptor binding yield information on drug affinity and efficacy? Biochem. Pharmacol. 60 (2000) 1549–1556.
[17] D.H. Williams, D.P. O'Brien, A.M. Sandercock, E. Stephens, Order changes within receptor systems upon ligand binding: receptor tightening/oligomerisation and the interpretation of binding parameters, J. Mol. Biol. 340 (2004) 373–383.